

ВЛИЯНИЕ МУТАЦИОННЫХ ВАРИАНТОВ СПАЙКОВОГО ГЛИКОПРОТЕИНА И РНК-ЗАВИСИМОЙ РНК-ПОЛИМЕРАЗЫ (nsp12) SARS-CoV-2 НА УЧАСТКИ СТЫКОВКИ С РЕМДЕСИВИРОМ

Давуд Али А.

Мосульсий университет, г. Мосул, Ирак

Резюме. В связи с быстрым развитием и эволюцией новых вариантов SARS-CoV-2 возникли проблемы, касающиеся их потенциального влияния на эффективность существующих вакцин. При этом наиболее значимые мутации касаются гена спайкового гликопротеина вируса. Ремдесивир, ингибирующий активность РНК-зависимой РНК-полимеразы (РдРп), является единственным препаратом, принятым FDA для лечения COVID-19 (nsp12). Исследовалось связывание (стыковка) гибкого лиганда (ремдесивира) с жесткими рецепторами (спайковый белок и РдРп). В ряде работ было обнаружено, что мутации спайкового гликопротеина и РдРп оказывают существенное влияние на поведение вируса и, в конечном счете, – на состояние здоровья человека. Показано, что позиция стыковки ремдесивира со спайковым белком и РдРп не определяется мутациями в недостающих петлях. Ремдесивир может связываться только с В- и С-цепями спайкового белка. Некоторые мутации могут передаваться в отдельных вариантах без изменения типа аминокислот, как, например, K417N, L452R, N501Y, D614G, T716I и S982A.

Ключевые слова: COVID-19, ремдесивир, РНК-зависимая РНК-полимераза, спайковый белок, мутации

INFLUENCE OF SARS-CoV-2 VARIANTS' SPIKE GLYCOPROTEIN AND RNA-DEPENDENT RNA POLYMERASE (nsp12) MUTATIONS ON REMDESIVIR DOCKING RESIDUES

Ali Adel Dawood

University of Mosul, Mosul, Iraq

Abstract. Rapid emergence and evolution of novel SARS-CoV-2 variants has raised concerns about their potential impact on efficiency of currently available vaccines. Among the most significant target mutations in the virus are those of the spike glycoprotein. Remdesivir, which inhibits the polymerase activity of the RNA-dependent RNA polymerase RdRp, is the only medicine approved by FDA for treatment of COVID-19 (nsp12). The docking features of the flexible ligand (remdesivir) with the stiff receptors was investigated in the present study (S protein and RdRp interaction). In various studies, the spike glycoprotein and RdRp mutations were found to have a significant influence upon viral behaviour and, as a result, affect human health. The docking position of remdesivir with the S and RdRp proteins was shown to be unaffected by mutations in the missing loops. The remdesivir can only bind the B and C chains of S protein. Some mutations can be transferred between variations, without changing the type of amino acid, such as K417N, L452R, N501Y, D614G, T716I, and S982A.

Keywords: COVID-19, remdesivir, RdRp, S protein, mutation

Адрес для переписки:

Али А. Давуд
Медицинский колледж Мосульского университета
Аль-Джамеа, 1, г. Мосул, Ирак.
Тел.: 00964 (770)-176-8002.
E-mail: aad@uomosul.edu.iq

Address for correspondence:

Ali A. Dawood
College of Medicine, University of Mosul
Al-Jameaa, st. 1, Mosul, Iraq.
Phone: 00964 (770)-176-8002.
E-mail: aad@uomosul.edu.iq

Образец цитирования:

Али А. Давуд «Влияние мутационных вариантов спайкового гликопротеина и РНК-зависимой РНК-полимеразы (nsp12) SARS-CoV-2 на участки стыковки с ремдесивиром» // Медицинская иммунология, 2022. Т. 24, № 3. С. 617-628.
doi: 10.15789/1563-0625-IOS-2486
© Давуд Али А., 2022

For citation:

Ali A. Dawood "Influence of SARS-CoV-2 variants' spike glycoprotein and RNA-dependent RNA polymerase (nsp12) mutations on remdesivir docking residues", *Medical Immunology (Russia)/Meditsinskaya Immunologiya*, 2022, Vol. 24, no. 3, pp. 617-628.
doi: 10.15789/1563-0625-IOS-2486
DOI: 10.15789/1563-0625-IOS-2486

Introduction

Despite the fact that COVID-19 has been vaccinated against by over half of the world's population, the virus continues to kill thousands of people and spread disease. Viral proteins have altered since the discovery of the Indian Delta variants, resulting in an increase in the number of cases. A novel coronavirus strain that produces COVID-19 has been the subject of press reports since December 2019. As a result of this, new varieties have been discovered, and they are being studied. Because it appears to be more easily transmitted from person to person, the CDC defines the delta coronavirus as a "variant" [24, 39]. As of July 2021, the SARS-CoV-2 Delta strain is the most infectious. Mutations that make a virus more dangerous, on the other hand, may hinder the virus from propagating efficiently [35].

In England, the B.1.1.7 lineage, B.1.617.2 in India, and B.1.351 in South Africa have all been identified as SARS-CoV-2 strains. Using all available resources, researchers are actively evaluating the efficacy of various medicines and vaccines against new strains with a range of escape mutations. It's unknown how these mutations influence SARS-CoV-2-host cell interactions in a systematic fashion, or if they increase morbidity [3, 26, 28]. As a result, creating broad-spectrum antiviral medicines and vaccines to tackle future SARS-CoV-2 strains will require a long-term clinical treatment strategy [1, 25].

The most important coronavirus protein is the spike protein. It's a viral transmembrane glycoprotein that helps the virus make contact with the host cell and invade it. The first protrudes from the surface of the viral particle and forms a corona-like halo. The functional components of the S protein are: S1 binds to cellular receptors on the surface of the host cell, such as ACE2, and S2 promotes cell-virus membrane fusion [32].

The viral RNA transcription and replication protein RNA-dependent RNA polymerase (nsp12) is responsible for the synthesis of viral RNA. The binding of nsp7 and nsp8 cofactors appears to be essential for SAR-CoV-2 RdRp RNA polymerase activity in order to increase RdRp binding and processivity (804 amino acids). RdRp's active site palm subdomain comprises polymerase motifs that are conserved, and its structure is comparable to those of other RNA polymerases. We chose these proteins in our study because of their relevance to the virus or the host cell [2, 15].

Any antiviral drug must target the component of the virus's life cycle that allows it to reproduce. Furthermore, a medicine must be capable of destroying viruses while causing no damage to the human cell that is infected. Viruses may also adapt to their surroundings. Because they reproduce so fast, they have a lot of opportunities to mutation (change their genetic code) with each new generation [9, 14].

Remdesivir (RDV) is an adenosine triphosphate analogue that was first discovered in 2017 to exhibit antiviral activity against the coronaviridae family. As a result, Remdesivir has sparked interest as a potential COVID-19 therapy. It has antiviral activity against numerous Ebola virus types in cell tests and monkey models. *In vitro* investigations show that Remdesivir reduces SARS-CoV by interfering with the polymerase activity of RNA-dependent RNA polymerase. Until October 2020, Remdesivir against COVID-19 was the only drug approved by the FDA. COVID-19 may be used to treat adults and adolescents aged 12 and above who weigh at least 88 pounds and have been hospitalised with COVID-19. Clinical trials suggest that Remdesivir may help these individuals recover more rapidly [12, 23, 36].

However, the molecular mechanism that allows for the maintenance of virulence is still mostly understood. We discuss how remdesivir binds to the S protein and RNA-dependent RNA polymerase (nsp12) in distinct viral strains, as well as the present state of knowledge. The goal of this research was to discover if new SARS-CoV-2 virus strains were spreading across countries. The discovery of SARS-CoV-2 variants might lead to more effective medicines, vaccines, and diagnostic tools. We investigated the development of novel SARS-CoV-2 variants with associated spike protein and RdRp mutations in a number of countries. Individual proteins with mutations at strategically important regions can alter the virus's biology [4, 15, 30, 38].

Materials and methods

In global stoichiometry with resolution 2.8, spike glycoprotein with ID (6VXX) was chosen from the PDB because it commonly lacks loops during the release process. The missing sequences were derived from the crystallographic information file's 6VXX wild type (CIF). With the discovery of the nonstructural protein (nsp12), also known as RdRp, as the primary component of the formally released protein from the RCBS PDB, this work was carried out (7OYG). The three-dimensional coordinate of the Remdesivir molecule was retrieved from the PubChem database. SARS-CoV-2 variants from different countries were chosen based on mutations in the S protein, as shown in Table 1.

Reconstruction missing loops of S protein

To determine the impact of missing loops in the S protein's interaction with the remdesivir, we used two methods to generate missing loops: creating sequences with Builder PyMOL software and utilizing a web application called ModLoop Queue. To determine the impact of missing loops in the S protein's interaction with the remdesivir, we used two methods to generate missing loops: creating sequences with Builder PyMOL software and utilizing

TABLE 1. WILD TYPE (6VXX) RESIDUES (R) COMPARED WITH 4 STRAINS OF SARS-CoV-2 IN DIFFERENT MUTATIONS

Name	Alt. Name	Detected	R 1	R 2	R 3	R 4	R 5	R 6	R 7	R 8
6VXX Wild type	QQZ48538	Mar 2020	<i>K417</i>	<i>L452</i>	<i>E484</i>	<i>N501</i>	<i>D614</i>	<i>P681</i>	<i>T716</i>	<i>S982</i>
Delta Indian variant	B.1.617.2	Dec 2020		<i>R452</i>	<i>Q484</i>		<i>G614</i>	<i>R681</i>		
UK variant	B.1.1.7	Feb 2020				<i>Y501</i>	<i>G614</i>	<i>H681</i>	<i>I716</i>	<i>A982</i>
South African variant	501Y.V2	Oct 2020	<i>N417</i>		<i>K484</i>	<i>Y501</i>	<i>G614</i>	<i>H681</i>	<i>I716</i>	<i>A982</i>
Brazilian variant	B.1.1.28.1	Dec 2020	<i>N417</i>		<i>K484</i>	<i>Y501</i>				

Note. Wild type residues = italic text. Mutation residues = bold italic text.

a web application called ModLoop Queue. Because the S protein is made up of three identical chains, the missing sequences were created in the same regions where mutations occurred and are listed in Table 1 for each variant. The starting missing loop (SER-469) is built on the C-terminal of the (ILE-468). Continuing residues were built on the following sequences: THR (470)-GLU-ILE-TYR-GLN-ALA-GLY-SER-THR-PRO-CYS-ASN-GLY-VAL-GLU-GLY-PHE-ASN-CYS (488). The CYS488 was built on the N-terminal of the TYR-489 residue. Another missing loop was started with GLN-677 which is built on the C-terminal of the residue (THR-676). The missing loop is GLN (677)-THR-ASN-SER-PRO-SER-GLY-ALA-GLY-SER-VAL-ALA. The last residue (ALA-688) was built on the N-terminal of the (SER-689) residue.

Molecular docking of remdesivir in the S and RdRp proteins

The binding location and impact of the antiviral medication (remdesivir triphosphate) with the SARS-CoV-2 S protein and RdRp were investigated using the AutoDock 4.2 molecular modelling simulation and PyRx protein ligand docking programmes. The interaction affinity as a scoring function was explored by docking protein molecules with remdesivir in a sequential manner. The docked complexes were visualized using UCSF Chimera and PyMOL. The interacting residues were investigated using the BIOVIA discovery studio. The built-in cavity identification method was used to identify potential binding locations. Each docking procedure was subjected to four runs. In addition, with a 100 Kcal/mol energy barrier, the maximum iterations were 1000. To identify the best conformations for each docking procedure, the lowest docked binding energy was employed [6, 8]. The missing hydrogen atoms were then added utilizing the BIOVIA discovery studio built-in technique, with specific attention paid to histidine (HIS) residues to add their H atoms depending on their microenvironment.

For the molecular simulation results, the five docking models with the highest binding energy and the most appropriate binding sites for a systematic

analysis of drug-S protein interactions were chosen. Based on protein structure, distribution characteristics, and polarity qualities of amino acid residues around the remdesivir molecule's binding sites, the molecular interaction technique and bioisosterism strategy were utilised to optimise three docking molecules. The new compounds created following optimization were simulated and evaluated using the same method, resulting in molecules with higher binding energies and tighter interactions. To test the accuracy of the remdesivir results, a short molecular dynamics (MD) simulation was run for each of the expected receptor-ligand complexes. The Molegro Virtual Docker was used to validate protein-ligand interactions and construct the molecular dock score and posture energy grid.

Results

Construction of missing loops

There is a clear contrast between the residues created using Builder PyMOL and ModLoop in the current investigation. As shown in Figure 1, the result clearly reveals that the ModLoop is more exact in distinguishing residue locations.

We found that remdesivir interacts with chain B of the S protein (6VXX) but not with chain A on multiple occasions, as shown in Figure 2. Following the loading of missing loops, we displayed changes to the Indian delta version of chain A. The most prevalent variant mutations in the S protein sequence in India are L452R, E484Q, D614G, and P681R. Other mutations are far away, whereas E484Q and P681R are located in the missing loops. Remdesivir (RDV) had no interaction with chain A, suggesting that the changes were unconnected. The magenta missing loops were created with the PyMOL builder, while the blue missing loops were created with ModLoop. D614G is closer to RDV's location than RDV is to D614G.

Molecular docking of the RDV with the B and C chains of S protein with missing loops

According to the current study, RDV has the strongest contact with the B and C chains of S protein. We performed RDV on the chain B of the UK variant

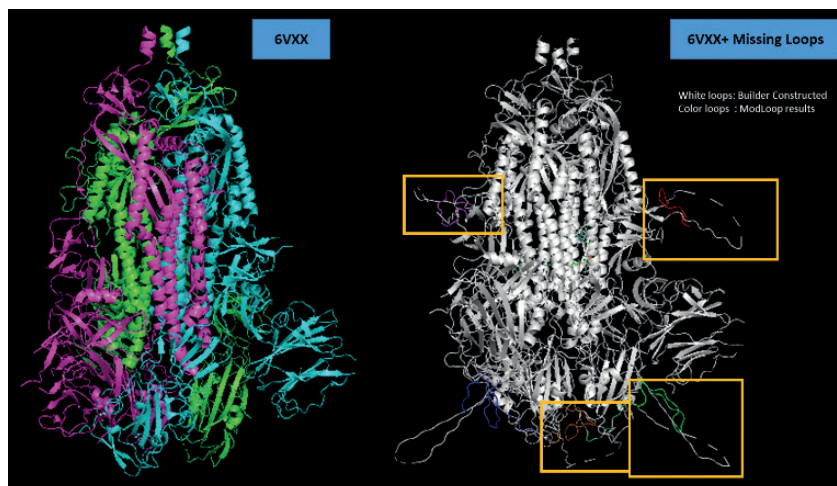


Figure 1. Crystal structure of S protein (6VXX)

Note. Left, cartoon structure shows three colored chains of wild 6VXX. Right, cartoon structure shows the missing loops: White loops constructed by Builder PyMOL. Colored loops constructed by ModLoop program.

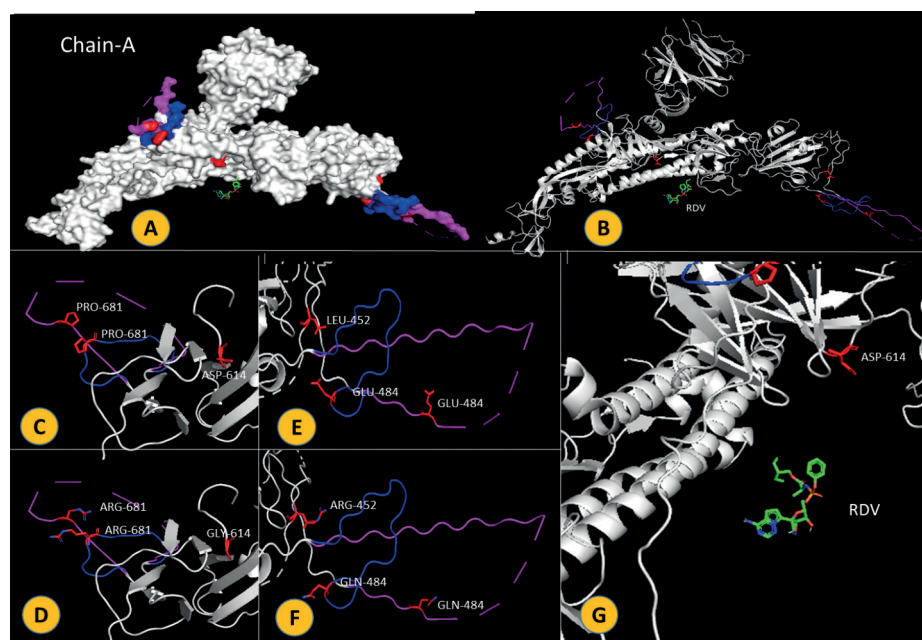


Figure 2. Chain A of S protein and its mutations show interaction with RDV

A, chain A surface view shows missing loops (colored). B, chain A cartoon view. C, Wild P681 (PRO-681) residue (magenta and blue) is in the missing loops and D614 (ASP-614) residue is in the main chain. D, mutated R681 (ARG-681) residue is in the missing loops and mutated G614 (GLY-614) residue is in the main chain. E, wild E484 (GLU-484) residue is in the missing loops and L452 (LEU-452) residue is in the main chain. F, mutated Q484 (GLN-484) residue is in the missing loops and R452 (ARG-452) residue is in the main chain. G, no docking was found between RDV and any residue in chain A.

S protein with the mutations after synthesizing the missing loops (N501Y, D614G, P681H, T716I, and S982A). Only the P681H mutation is present in the missing loops. Figures 3, 4 show that S982A is closer to the RDV docking point as a result of this outcome. The RDV docking pose with the S protein chains B and C revealed conventional hydrogen bonds in the residues (B: ARG-1014, C: ARG-765, GLY769, and LEU-1012), as well as a new hydrogen bond in the

C: GLN-762 residue, an unfavorable positive bond (red), a pi-sigma bond in the B: ALA-958 residue, and a pi-alkyl bond in the B: ALA-958 residue. Binding affinity and root-mean-square distance (RMSD) were calculated to choose the best pose with upper and lower RMSD. The best selected docking model is the first one when the RMSD/up, lb is equal to zero and the binding affinity is (-5.9). The first and third models have the highest MoleDock scores (-116.29

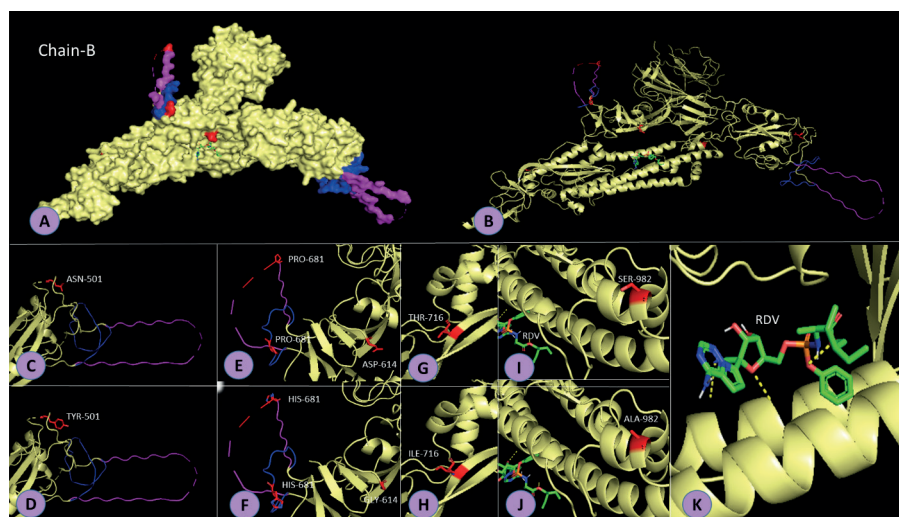


Figure 3. Molecular docking of RDV with chain B of the wild and mutation residues

Note. A, RDV interacts with the chain B surface view and shows missing loops (colored). B, chain B ribbon view with RDV docking (green color). C, N501 (ASN-501) wild residue is in the main chain and the missing loops (magenta and blue). D, mutated Y501 (TYR-501) residue is in the main chain with the missing loops. E, wild P681 (PRO-681) residue (magenta and blue) is in the missing loops and D614 (ASP-614) residue is in the main chain. F, mutated H681 (HIS-681) residue is in the missing loops and mutated G614 (GLY-614) residue is in the main chain. G, wild T716 (THR-716) residue. H, mutated I716 (ILE-716) residue. I, wild S982 (SER-982) residue is closer to the RDV docking. J, mutated A982 (ALA-982) residue. K, interaction between RDV and S protein (chain B).

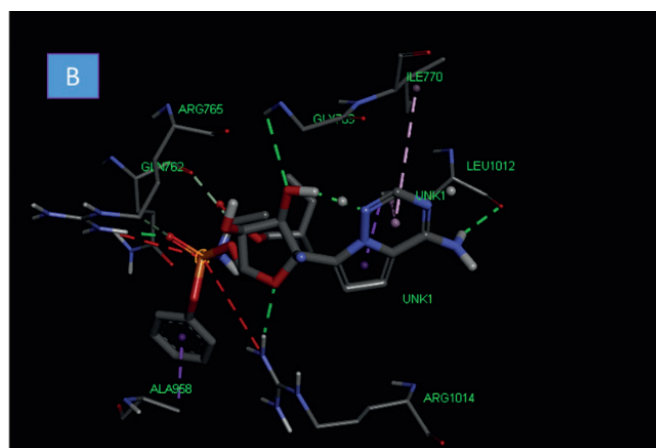
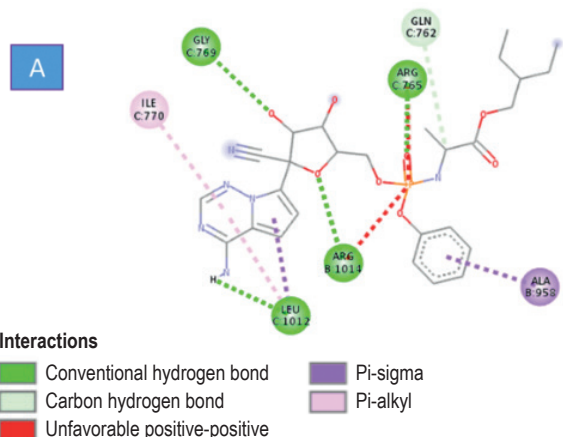


Figure 4. Molecular docking of remdesivir (RDV) with the S protein

Note. A, 2D pose docking shows conventional hydrogen bonds ARG-1014 residue is in the chain B and (ARG-765, GLY-769, and LEU-1012) residues are in the chain C (green), new hydrogen bond of GLN-762 residue is in chain C (grey), unfavorable positive bond (red), Pi-sigma bond is in the ALA-958 residue of the chain B (purple), and Pi-alkyl bond is in the ILE-770 residue in the chain C (magenta). B, RDV-6VXX interactions in the 3D structure.

and -120.287 respectively). The best protein-ligand gird score is showed with the first model (-74.4338) and the highest Rerank score (-113.599) of the fourth model. This interaction formed 4 conventional H-bonds with B: ARG-1014, C: ARG-765, GLY-769, and LEU-1014. A novel hydrogen bond was formed with C: GLN-762. Molegro Virtual Docker was used to predict ligand scores such as Grid, MolDock, and Rerank, Table 2. The best energy pose is under -40, Figure 5.

Following the construction of the missing loops, we performed RDV on chain C of the S protein of the South African variety with mutations (K417N, E484K, N501Y, D614G, P681H, T716I, and S982A). The missing loops contain mutations E484K and P681H. All mutations are far from the fusion. The RDV docking position is shared by Chains B and C, as shown in Figure 6.

After modeling the missing loops, we performed RDV on the chain B of the S protein of the Brazilian version with mutations (K417N, E484K, and

TABLE 2. BINDING AFFINITY, UPPER BOUND RMSD/ub AND LOWER BOUND RMSD/lb DEGREE OF THE TOP OF INTERACTION MODELS BETWEEN RVD AND S PROTEIN EXTRACTED BY PyRx

6VXX-RDV	Binding Affinity	RMSD/ub	RMSD/lb	GRID Score	MolDock Score	Rerank Score
6VXX_121304011_uff_E = 1044.71	-5.9	0	0	-74.4338	-116.29	-96.6824
6VXX_121304012_uff_E = 1044.71	-4.5	13.996	9.456	-73.9069	-108.534	-98.4069
6VXX_121304013_uff_E = 1044.71	-4.5	17.778	12.044	-65.0775	-91.9958	-80.1375
6VXX_121304014_uff_E = 1044.71	-4.4	13.858	10.585	-64.7753	-120.287	-113.599
6VXX_121304015_uff_E = 1044.71	-4.4	17.451	11.529	-60.6775	-104.732	-85.1287

Note. Grid, MolDock, and Rerank were estimated by Molegro Virtual Docker.

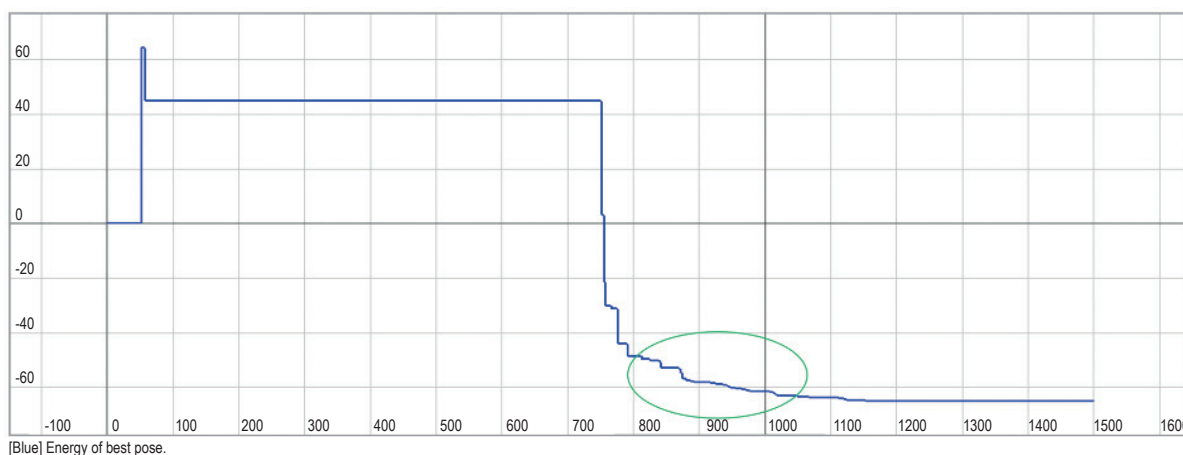


Figure 5. Schematic graph shows the energy poses the blue line of 6VXX-RDV interaction extracted from Molegro Virtual Docker

Note. The best docking score is in the green circle.

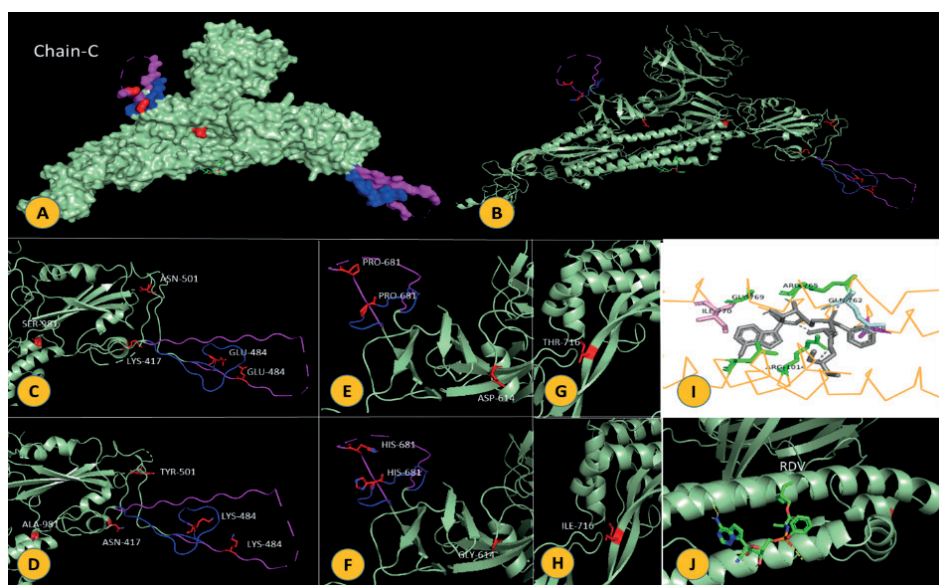


Figure 6. RDV-Chain C docks in the wild and mutation residues

Note. A, RDV interacts with the chain C surface view and shows missing loops (colored). B, chain C ribbon view with RDV docking (green color). C, N501 (ASN-501), S981 (SER-981), and K417 (LYS-417) wild residues are in the main chain and E484 (GLU-484) residue is in the missing loops (magenta and blue). D, mutated Y501 (TYR-501), A981 (ALA-981), and N417 (ASN-417) residues are in the main chain and K484 (LYS-484) residue is in the missing loops. E, wild P681 (PRO-681) residue (magenta and blue) is in the missing loops and D614 (ASP-614) residue is in the main chain. F, mutated H681 (HIS-681) residue is in the missing loops and mutated G614 (GLY-614) residue is in the main chain. G, wild T716 (THR-716) residue. H, mutated I716 (ILE-716) residue. I, RDV interacts with the C chain residues (ILE-770, GLY-769, ARG-765, GLN-762, ARG-1014, and ALA-958). J, RDV-6VXX chain C interaction cartoon view.

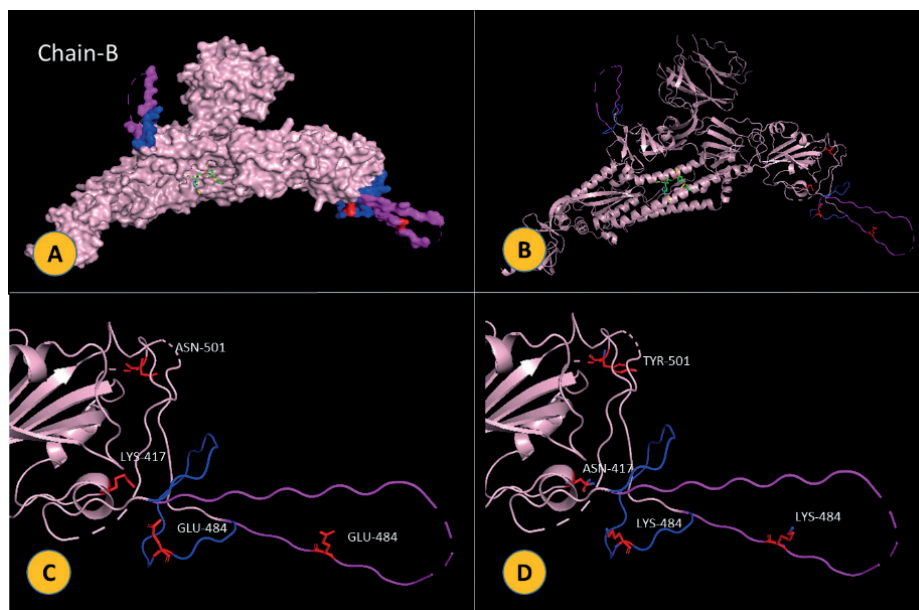


Figure 7. RDV-Chain B interactions of wild and mutation residues

Note. A, RDV interacts with the chain B surface view and shows missing loops (colored). B, chain B ribbon view with RDV docking (green color). C, N501 (ASN-501) and K417 (LYS-417) wild residues are in the main chain and wild E484 (GLU-484) is in the missing loops (magenta and blue). D, mutated Y501 (TYR-501) and N417 (ASN-417) residues are in the main chain and mutated K484 (LYS-484) residue is in the missing loops.

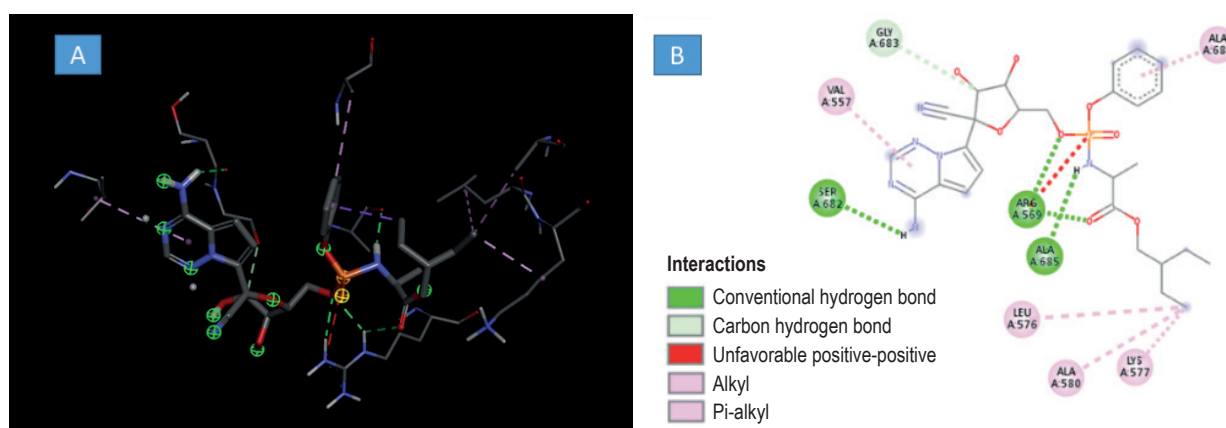


Figure 8. Molecular docking pose of RDV-RdRp

Note. A, the crystal structure of the pose interaction shows the colored bonds. B, 2D structure of molecular atoms interaction shows 3 conventional-hydrogen green bonds (A: ARG-569, SER-682, and ALA-685). A novel carbon hydrogen grey bond (A: GLY-683). 3 alkyl pale magenta bonds (A: LEU-576, LYS-577, and ALA-580). Pi-alkyl dark magenta bond (A: ALA-688).

N501Y). In the missing loops, the E484K mutation is discovered. Figure 7 shows how all mutations are situated far away from the docking stance.

Molecular docking of the RDV with RdRp (nsp12)

RDV has an excellent fusion with RdRp, it has been discovered. Rerecording of the most applicable bonds: Figure 8 shows three conventional hydrogen bonds (ARG-569, SER-682, and ALA-685), a new carbon-hydrogen bond (A: GLY-683), three alkyl bonds (A: LEU-576, LYS-577, and ALA-580), a Pi-alkyl bond (A: ALA-688) and an unfavourable positive-positive interaction with the residue (A:

ARG-569). The top five docking models were chosen based on their greatest binding affinity and lowest RMSD/ub, lb characteristics. The first model has the highest binding affinity when the RMSD equal to zero. Not only that but the MolDock score for the first model is considered the highest (-100.334) with the GRID score (-51.3551) but the Rerank score is less than other models (-19.4025). The lowest MolDock score related to the fourth model with the GRID and Rerank score -27.9188, -29.6737 respectively, Table 3. The best energy pose is under -40, Figure 9. Only one mutation has been determined in the RdRp (P323L).

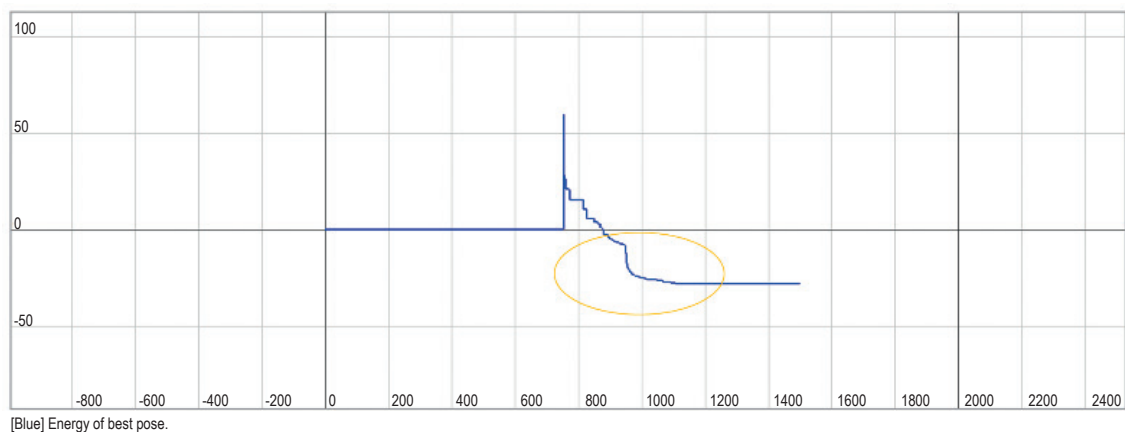


Figure 9. Schematic graph shows the energy poses the blue line of RdRp-RDV interaction extracted from Molegro Virtual Docker

Note. The best docking score is in the orange circle.

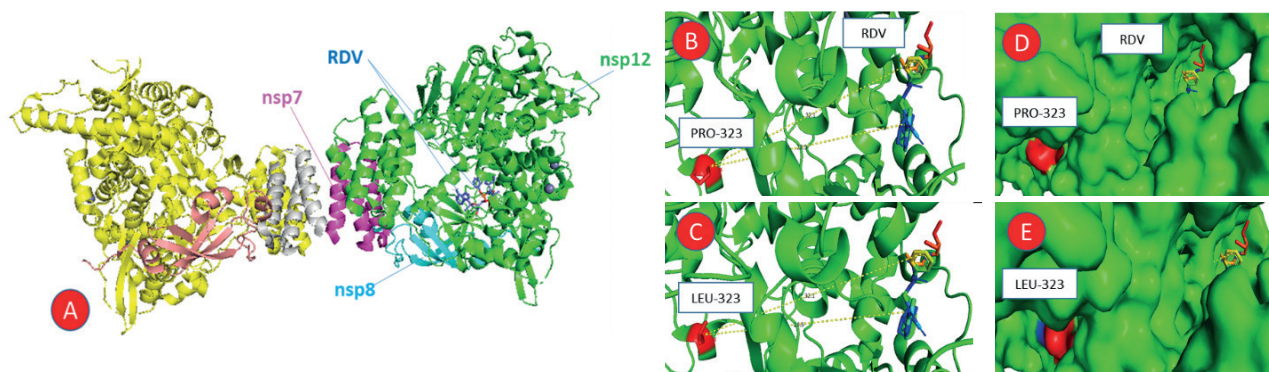


Figure 10. RDV-RdRp docks of wild and mutation residues

Note. A, RDV interacts with the nsp12 cartoon view. B, wild P323 (PRO-323) residue in the nsp12 is closer to the RDV docking site (blue). C, mutated L323 (LEU-323) residue. D, wild P323 (PRO-323) residue shows the surface view. E, mutated L323 (LEU-323) residue shows the insider pocket in the surface view.

TABLE 3. BINDING AFFINITY, UPPER BOUND RMSD/ub AND LOWER BOUND RMSD DEGREE OF THE TOP OF INTERACTION MODELS BETWEEN RVD AND RdRp EXTRACTED BY PyRx

RdRp-RDV	Binding Affinity	RMSD/ub	RMSD/lb	GRID Score	MolDock Score	Rerank Score
nsp12_121304011_E = 1044.71	-7.4	0	0	-51.3551	-100.334	-19.4025
nsp12_121304012_E = 1044.71	-7.3	31.6	28.094	-36.4412	-94.5294	-11.1266
nsp12_121304016_E = 1044.71	-7.1	53.41	50.312	-33.0435	-63.576	-42.8843
nsp12_121304014_E = 1044.71	-7	31.565	28.01	-27.9188	-37.6395	-29.6737
nsp12_121304015_E = 1044.71	-6.9	4.623	2.491	-24.3764	-73.0735	-31.9112

Note. Grid, MolDock, and Rerank were estimated by Molegro Virtual Docker.

With the RDV, the distance between the mutation site and the docking posture is randomly assessed at 28.5 and 32.1. In the current investigation, there was no difference in the distance between natural and mutant RdRp and RDV residues. There are no evident structural variations in RdRp structure between the wild and mutant forms, as shown in Figure 10.

Discussion

The worldwide economy and health system have been hit by the COVID-19 outbreak like never before. SARS-CoV-2 has a high level of transmissibility and tissue tropism in a wide range of tissues [29, 32].

This study focused on interventional treatments that target the SARS-CoV-2 viral entry machinery, such as spike protein or RdRp. Several remedies have recently been proposed and are receiving considerable investigation, including small-molecule medicines, antibodies, and antiviral peptides. At the molecular level, SARS-CoV-2 interactions with any medicine are investigated, and this information is critical for prevention and treatment. A variety of trajectories from long molecular dynamics (MD) simulations of the SARS-CoV-2 S protein are now available in the public domain [5, 7, 13, 20, 21].

The most prevalent share mutations in all of the selected nations are E484Q (K), D614G, and P681R (H), according to an analysis of the mutations in the various variants of the virus under study. When it comes to constructing missing loops, the ModLoop Queue software outperforms Builder PyMol. According to our findings, the fusion position of the remdesivir is restricted to the B and C chains within the following residues: B-(A958 and R1014), C-(Q762, R765, G769, I770, and L1012) respectively. Despite the presence of weak carbon-hydrogen bonds and unfavorable bonds as a result of the docking (6VXX-RDV), the binding affinity and electrostatic energy were high.

In the missing loops, the delta Indian version contains two out of four mutations: E484Q and P681R (50 percent), but the UK variation only has one out of five mutations: P681H. (20%). In the missing loops, the South African version has two out of seven mutations: E484K and P681H (28.5%), whereas the Brazilian variant has one out of three mutations: E484K. (33.3%). Extrapolating the data, it becomes evident that the missing loops include roughly half of the mutations discovered in the variants. Our study found that mutations in the missing loops did not influence on the docking location of the remdesivir with S protein. The most common mutation with the COVID-19 variants is D614G. D614G is thought to provide for a more open S protein structure, which is better for ACE2 interaction [19, 33]. The findings demonstrate that some mutations, including K417N, L452R, N501Y, D614G, T716I, and S982A, can be passed down between variants without altering the

type of amino acid. In the delta Indian variations, glutamate (E) is changed to glutamine (Q), whereas in South African and Brazilian variants, glutamate (E) is changed to lysine (K). In delta Indian variant, the proline is changed to arginine, while in the UK and South African variants, the proline is changed to histidine.

RdRp is a key target for antiviral medication development against a variety of viruses. Three RdRp inhibitors have been proposed as possible targets for SARS-CoV-2 infection: favipiravir, galidesivir, and remdesivir [19, 22, 27, 33, 36, 37]. Understanding the molecular mechanism of remdesivir's interaction with RdRp, as well as other potential targets, is critical for COVID-19 treatment development [27, 36, 37].

Although it's been speculated that the RdRp P323L mutation affects viral proofreading, resulting in a greater prevalence of downstream mutations, it's attracted less attention. According to a recent study, the RdRp mutation began to become more widespread in European viral genomes on February 20, 2020, and is associated with a greater frequency of point mutations than in Asian viral genomes. In a hydrophobic cleft near the changed P323L residue, which corresponds to mutation 14408 in the current study, a possible docking site was revealed. Drug resistance can be caused by naturally occurring mutations in RdRp, as has been previously documented [17, 22, 31, 34]. Although additional research is required to determine the underlying molecular significance of the mutations, we believe that the P323L mutation reduces the clinical manifestation of SARS-CoV-2.

It also has a high binding affinity for RdRp, which was confirmed in the current study. According to new study, RDV can bind RdRp. In the (apo) form or in combination with the RNA template primer, SARS-CoV-2 RdRp can bind to RDV. RDV binds to Mpro efficiently, according to current *in silico* studies, corroborating our idea. RDV was also shown to be more efficient than lopinavir/ritonavir *in vitro* and in MERS-CoV-infected mice. Remdesivir was revealed to have a considerable affinity for the SARS-CoV-2 virus's main protease [10, 11]. When the RMSD/ub, lb was equal to zero in the first model, the binding affinity of the RDV with the RdRp was very high in the current investigation. This docking gave the higher MolDock and GRID scores compared to the rest of the models. Furthermore, we noticed that the P323L mutation did not effect on the remdesivir docking site. The RdRp wild and mutant types had similar distances between the docking location and the P323L residue.

The improved molecules, according to molecular simulations, have a higher binding energy and may interact with a greater number of amino acid residues in a variety of ways, resulting in unfavourable interactions [16, 18]. In both molecular dynamics datasets, the primary interactions are different,

with protomers working to follow the oligomer's symmetry. Because remdesivir docks with the B and C chains of S protein, we expect the mutations to disrupt the connections that link the AC, CB, and BA chains. Overall, our findings reveal that mutations in the S protein promote enhanced infectivity in cellular systems and, using molecular modelling, provide a structural foundation for this effect. RdRp demonstrated a greater affinity for Remdesivir than S protein, and the two formed an unstable complex.

Conclusions

The most prevalent share mutations in all of the selected variants are E484Q (K), D614G, and P681R (H). Spike glycoprotein and RdRp mutations were shown to have a substantial impact on viral behavior

and, as a result, human health in several investigations. Our study found that mutations in the missing loops did not influence on the docking location of the remdesivir with S and RdRp proteins. The docking position of the remdesivir is restricted to the B and C chains of the S protein. The findings demonstrate that some mutations, including K417N, L452R, N501Y, D614G, T716I, and S982A, can be passed down between variants without altering the type of amino acid. Furthermore, we noticed that the P323L mutation did not effect on the remdesivir docking site. RdRp exhibited a greater affinity for remdesivir than S protein, and both formed an unstable complex.

Acknowledgments

The author thanks college of Medicine for documenting this paper.

References

1. Baum A., Fulton B.O., Wloga E., Copin R., Pascal K.E., Russo V., Giordano S., Lanza K., Negron N., Ni M., Wei Y., Atwal G.S., Murphy A.J., Stahl N., Yancopoulos G.D., Kyratsos C.A. Antibody cocktail to SARS-CoV-2 spike protein prevents rapid mutational escape seen with individual antibodies. *Science*, 2020, Vol. 369, pp. 1014-1018.
2. Choy K.-T., Wong A.Y.-L., Kaewpreedee P., Sia S.F., Chen D., Hui K.P.Y., Chu D.K.W., Chan M.C.W., Cheung P.P.-H., Huang X., Peiris M., Yen H.-L. Remdesivir, lopinavir, emetine, and homoharringtonine inhibit SARS-CoV-2 replication *in vitro*. *Antiviral Res.*, 2020, Vol. 178, 104786. doi: 10.1016/j.antiviral.2020.104786.
3. Dawood A., Altobje M., Alnori H. Compatibility of the ligand binding sites in the spike glycoprotein of covid-19 with those in the aminopeptidase and the caveolins 1, 2 proteins. *Res. J. Pharm. Tech.*, 2021, Vol. 14, no. 9, pp. 4760-4766.
4. Dawood A., Altobje M., Alrassam Z. Molecular docking of SARS-CoV-2 nucleocapsid protein with angiotensin-converting enzyme II. *Mikrobiol. Zhu*, 2021, Vol. 83, no. 2, pp. 82-92.
5. Dawood A., Altobje M. Inhibition of N-linked glycosylation by nunicamycin may contribute to the treatment of SARS-CoV-2. *Microbiol. Path.*, 2020, Vol. 149, 104586. doi: 10.1016/j.micpath.2020.104586.
6. Dawood A. Glycosylation, ligand binding sites and antigenic variations between membrane glycoprotein of COVID-19 and related coronaviruses. *Vacunas*. 2021, Vol. 22, no. 1, pp. 1-9.
7. Dawood A. Identification of CTL and B-cell epitopes in the Nucleocapsid Phosphoprotein of COVID-19 using Immunoinformatics. *Microbiol. J.*, 2021, Vol. 83, no. 1, pp. 78-86.
8. Dawood A. New variant of SARS-CoV-2 in South Africa. *Prog. Med. Sc.*, 2021, Vol. 5, no. 1, pp. 1-2.
9. Dawood A. Using remdesivir and dexamethasone for treatment of SARS-CoV-2 shortens the patient's stay in the hospital. *Asi an J. Pharm. Res.*, 2021, Vol. 11, Iss. 2, 138-0. doi: 10.52711/2231-5691.2021.00026.
10. Deshpande R., Tiwari P., Nyayanit N., Modak M. In silico molecular docking analysis for repurposing therapeutics against multiple proteins from SARS-CoV-2. *Eur. J. Pharmacol.*, 2020, Vol. 886, 173430. doi.org/10.1016/j.ejphar.2020.173430.
11. Eskier D., Karakulah G., Suner A., Oktay Y. RdRp mutations are associated with SARS-CoV-2 genome evolution. *Peer J.*, 2020, Vol. 8, e9587. doi:/10.7717/peerj.9587.
12. Eweas A., Alhossary A., Abdul-Moneim A. Molecular Docking Reveals ivermectin and remdesivir as potential repurposed drugs against SARS-CoV-2. *Front. Microbiol.*, 2021, Vol. 11, e592908. doi: 10.3389/fmicb.2020.592908.
13. Garvin M.R., Prates E.T., Pavicic M., Jones P., Amos B.K., Geiger A., Shah M.B., Streich J., Gazolla J.G.F.M., Kainer D., Cliff A., Romero J., Keith N., Brown J.B., Jacobson D. Potentially adaptive SARS-CoV-2 mutations discovered with novel spatiotemporal and explainable AI models. *Genome Biol.*, 2020, Vol. 21, 304. doi: 10.1186/s13059-020-02191-0.
14. Grein J., Ohmagari N., Shin D., Diaz G., Asperges E. Compassionate use of remdesivir for patients with severe Covid-19. *N. Engl. J. Med.*, 2020, Vol. 382, pp. 2327-2336.
15. Hall Jr., Ji H-F. A search for medications to treat COVID-19 via in silico molecular docking models of the SARS-CoV-2 spike glycoprotein and 3CL protease. *Travel Med. Infect. Dis.*, 2020, Vol. 35, 101646. doi: 0.1016/j.tmaid.2020.101646.
16. Henderson R., Edwards R.J., Mansouri K., Janowska K., Stalls V., Gobeil S.M.C., Kopp M., Li D., Parks R., Hsu A.L., Borgnia M.J., Haynes B.F., Priyamvada acharya controlling the SARS-CoV-2 spike glycoprotein conformation. *Nat. Struct. Mol. Biol.*, 2020, Vol. 27, pp. 925-933.

17. Ilmjärv S., Abdul F., Acosta-Gutiérrez S., Estarellas C., Galdadas I., Casimir M., Alessandrini M., Gervasio F.L., Krause K.-H. Concurrent mutations in RNA-dependent RNA polymerase and spike protein emerged as the epidemiologically most successful SARS-CoV-2 variant. *Sci. Rep.*, 2021, Vol. 11, 13705. doi: 10.1038/s41598-021-91662-w.
18. Jean S., Lee I., Hsueh R. Treatment options for COVID-19: the reality and challenges. *J. Microbiol. Immunol. Infect.*, 2020, Vol. 53, pp. 436-443.
19. Kumar Y., Singh H., Patel C.N. In silico prediction of potential inhibitors for the main protease of SARS-CoV-2 using molecular docking and dynamics simulation based drug-repurposing. *J. Infect. Public Health*, 2020, Vol. 13, pp. 1210-1223.
20. Mari A., Roloff T., Stange M., Søgaaard K.K., Asllanaj E., Tauriello G., Alexander L.T., Schweitzer M., Leuzinger K., Gensch A., Martinez A.E., Bielicki J., Pargger H., Siegemund M., Nickel C.H., Bingisser R., Osthoff M., Bassetti S., Sendi P., Battegay M., Marzolini C., Seth-Smith H.M.B., Schwede T., Hirsch H.H., Egli A. Global genomic analysis of SARS-CoV-2 RNA dependent RNA polymerase evolution and antiviral drug resistance. *Microorganisms*, 2021, Vol. 9, no. 5, 1094. doi: 10.3390/microorganisms9051094.
21. Nguyen H., Thai N., Truong D., Li M. Remdesivir Strongly Binds to Both RNA-Dependent RNA polymerase and Main Protease of SARS-CoV-2: Evidence from Molecular Simulations. *J. Phys. Chem.*, 2020, Vol. 124, pp. 11337-11348.
22. Pachetti M., Marini B., Benedetti F., Giudici F., Mauro E., Storici P., Masciovecchio C., Angeletti S., Ciccozzi M., Gallo R.C., Zella D., Ippodrino R. Emerging SARS-CoV-2 mutation hot spots include a novel RNA-dependent-RNA polymerase variant. *J. Transl. Med.*, 2020, Vol. 18, no. 1, 179. doi.org/10.1186/s12967-020-02344-6.
23. Sada M., Saraya T., Ishii H., Okayama K., Hayashi Y., Tsugawa T., Nishina A., Murakami K., Kuroda M., Ryo A., Kimura H. Detailed molecular interactions of favipiravir with SARS-CoV-2, SARS-CoV, MERS-CoV, and influenza virus polymerases in silico. *Microorganisms*, 2020, Vol. 8, no. 10, 1610. doi: 10.3390/microorganisms8101610.
24. Salleh M.Z., Derrick J.P., Deris Z.Z. Structural evaluation of the spike glycoprotein variants on SARS-CoV-2 transmission and immune evasion. *Inter. J. Mol. Sci.*, 2021, Vol. 22, no. 14, 7425. doi.org/10.3390/ijms22147425.
25. Senger M.R., Evangelista T.C.S., Dantas R.F., Santana M.V.D.S., Gonçalves L.C.S., de Souza Neto L.R., Ferreira S.B., Silva-Junior F.P. COVID-19: molecular targets, drug repurposing and new avenues for drug discovery. *Mem. Inst. Oswaldo Cruz*, 2020, Vol. 115, e200254. doi: 10.1590/0074-02760200254.
26. Shaen A., Sattar N., Ibrahim M., Irfan M. Role of Remdesivir in COVID-19. *Aus. J. Pulm. Res. Med.*, 2021, Vol. 8, no. 1, 1071.
27. Sheahan T.P., Sims A.C., Leist S.R., Schafer A., Won J. Comparative therapeutic efficacy of remdesivir and combination lopinavir, ritonavir, and interferon beta against MERS-CoV. *Nat. Commun.*, 2020, Vol. 11, no. 1, 222. doi: 10.1038/s41467-019-13940-6.
28. Shehroz M., Zaheer T., Hussain T. Computer-aided drug design against spike glycoprotein of SARS-CoV-2 to aid COVID-19 treatment. *Heliyon*, 2020, Vol. 6, no. 10, e05278. doi.org/10.1016/j.heliyon.2020.e05278.
29. Showers W., Leach S., Kechris K., Strong M. Analysis of SARS-CoV-2 Mutations over time reveals increasing prevalence of variants in the spike protein and RNA-dependent RNA polymerase. *bioRxiv*, 2021. doi: 10.1101/2021.03.05.433666.
30. Sun C., Zhang J., Wei J., Zheng X., Zhao X., Fang Z., Xu D., Yuan H., Liu Y. Screening, simulation, and optimization design of small molecule inhibitors of the SARS-CoV-2 spike glycoprotein. *PLoS One*, 2021, Vol. 16, no. 1, e0245975. doi: 10.1371/journal.pone.0245975.
31. Walls C., Park Y.-J., Tortorici A., Wall A., McGuire T., Veesler D. Structure, function, and antigenicity of the SARS-CoV-2 spike glycoprotein. *Cell*, 2020, Vol. 181, pp. 281.e6-292.e6.
32. Wang M., Cao R., Zhang L., Yang X., Liu J., Xu M., Shi Z., Hu Z., Zhong W., Xiao G. Remdesivir and chloroquine effectively inhibit the recently emerged novel coronavirus (2019-nCoV) in vitro. *Cell Res.*, 2020, Vol. 30, pp. 269-271.
33. Williamson B.N., Feldmann F., Schwarz B., Meade-White K., Porter D.P., Schulz J., van Doremalen N., Leighton I., Yinda C.K., Pérez-Pérez L., Okumura A., Lovaglio J., Hanley P.W., Saturday G., Bosio C.M., Anzick S., Barbian K., Cihlar T., Martens C., Scott D.P., Munster V.J., de Wit E. Clinical benefit of remdesivir in rhesus macaques infected with SARS-CoV-19. *Nature*, 2020, Vol. 585, pp. 273-276.
34. Wu A., Peng Y., Huang B., Ding X., Wang X., Niu P., Meng J., Zhu Z., Zhang Z., Wang J., Sheng J., Quan L., Xia Z., Tan W., Cheng G., Jiang T. Genome composition and divergence of the novel coronavirus (2019-nCoV) originating in China. *Cell Host Microbe*, 2020, Vol. 27, pp. 325-328.
35. Wu C., Chen X., Cai Y., Xia J., Zhou X. Risk factors associated with acute respiratory distress syndrome and death in patients with coronavirus disease 2019 pneumonia in Wuhan, China. *JAMA Intern. Med.*, 2020, Vol. 180, no. 7, pp. 1-11.
36. Yin W., Mao C., Luan X., Shen D.-D., Shen Q., Su H., Wang X., Zhou F., Zhao W., Gao M., Chang S., Xie Y.C., Tian G., Jiang H.-W., Tao S.-C., Shen J., Jiang Y., Jiang H., Xu Y., Zhang S., Zhang Y., Xu H.E. Structural basis for inhibition of the RNA-dependent RNA polymerase from SARS-CoV-2 by remdesivir. *Science*, 2020, Vol. 368, pp. 1499-1504.
37. Yurkovetskiy L., Wang X., Pascal K.E., Tomkins-Tinch C., Nyalile T.P., Wang Y., Baum A., Diehl W.E., Dauphin A., Carbone C., Veinotte K., Egri S.B., Schaffner S.F., Lemieux J.E., Munro J.B., Rafique A., Barve A.,

Sabeti P.C., Kyratsous C.A., Dudkina N.V., Shen K., Luban J. Structural and functional analysis of the D614G SARS-CoV-2 spike protein variant. *Cell*, 2020, Vol. 183, pp. 739-751.e8.

38. Zhang Q., Xiang R., Huo S., Zhou Y., Jiang S., Wang Q., Yu F. Molecular mechanism of interaction between SARS-CoV-2 and host cells and interventional therapy. *Sig. Transduct. Target. Ther.*, 2021, Vol. 6, no. 1, 233. doi: 10.1038/s41392-021-00653-w.

39. Zhu N., Zhang D., Wang W., Li X., Yang B., Song J., Zhao X., Huang B., Shi W., Lu R., Niu P., Zhan F., Ma X., Wang D., Xu W., Wu G., Gao G.F., Tan W. A novel coronavirus from patients with pneumonia in China, 2019. *N. Engl. J. Med.*, 2020, Vol. 382, pp. 727-733.

Автор:

Али А. Давуд – к.микробиол.н., лектор, кафедра анатомии Медицинского колледжа Мосульского университета, г. Мосул, Ирак

Author:

Ali A. Dawood, PhD (Microbiology), Lector, Department of Anatomy, College of Medicine, University of Mosul, Mosul, Iraq

Поступила 16.03.2022
Принята к печати 30.03.2022

Received 16.03.2022
Accepted 30.03.2022